ATLANTIS PRESS

Advances in Computer Science Research, volume 93

2nd International Conference on Mathematics, Modeling and Simulation Technologies and Applications (MMSTA 2019)

3D Source Generation Method for Integrated Imaging

Zesheng Liu[1], Hui Deng[2,*], Yuefei Su[1], Liangshuo Du[1] and Yongcong Zhang[1]

[1]School of Network & Communication Engineering, Chengdu Technological University, Chengdu 611730, China

[2]School of Electronic Engineering, Chengdu Technological University, Chengdu 611730, China

[*]Corresponding author

***Abstract*—This paper proposed a 3D source generation method for generating elemental image array (EIA) of integrated imaging. The proposed method can break through the constraints between parameters of traditional integrated imaging record device and display device, and allow to obtain a new set of EIA suited to be displayed by an integrated imaging display device with arbitrary parameters from any given recorded EIA. Three-dimensional display results demonstrate the correctness and effectiveness of the proposed method.**

Keywords—integrated imaging; elemental image array

I. INTRODUCTION

Integrated imaging, as currently a main research direction in three-dimensional (3D) display areas [1-4], is considered to be the most promising techniques to bring 3D display to films and television. Since firstly proposed by Lipmann in 1908, integrated imaging has encountered the depth reversal problem [5-6], and researchers have always worked on overcoming this drawback [7-9]. A simple but effective method proposed by Okano and co-workers is to rotate each elemental image by 180º around the image center [10], but it still has a weakness of reconstructing only virtual 3D images. Another classical method which carries out a second record process was proposed by H. E. Ives [6], the depth of reconstructed 3D image is reversed twice, so an orthoscopic image with correct depth can be obtained. With the development of computer techniques, computerized two-step integrated imaging methods were proposed [11-14], the second record process of Ives' method is simulated in computer and synthetic elemental image array (EIA) is generated by pixel mapping algorism, integrated imaging display using these methods can avoid the problem of image quality degrading which is generally existed in the optical record methods [15]. However, consequent problems such as black zone, pixel mapping errors, and homologous pixels missing are discovered in pixel mapping process. To solve these problems, methods of eliminating black zone and methods of decreasing pixel mapping errors were proposed [16-18]. A major requisite for applying integrated imaging to 3D films and television is the generation of 3D source with corresponding parameters to match various display devices. Integrated imaging is theoretically based on the path-reversal principle, it requires the same parameters in both record and display processes to reconstruct the real light field of the object. But 3D display devices of integrated imaging systems vary in their parameters Therefore, greater demands are being placed on the methods of generating synthetic EIA.

In this paper we propose a 3D source generation method to generate, according to the parameters of integrated imaging display device, the synthetic EIA from the one captured in the record process of integrated imaging. Integrated imaging system using this method can realize the aim of "record once and display everywhere" by generating the synthetic EIA which matches the display device with different lens array, different displaying mode (depth-priority mode or resolution-priority mode), different 3D viewing angle and different resampling spacing (larger or smaller than the sample spacing in the record process).

II. PRINCIPLES

The proposed EIA generation method, as shown in Figure 1, consists of two steps which are 3D-coordinates restoration and EIA resampling. Two pinhole arrays (PA): PA1 and PA2 are set up to simulate the record lens array and display lens array, respectively. Rays emitted from each set of homologous pixels of EIA1 (captured in the record process) are converged as a 3D image point, the 3D coordinates of each 3D object point can be restored by simple geometric calculation with parameters of EIA1 and PA1. Synthetic EIA2 can be obtained by resampling the 3D point through the PA2. The EIA2 generated with this method can break through the constraints of sampling spacing and sampling range of the record lens array in an integrated imaging system, this makes the synthetic EIA2 with smaller sampling spacing and larger sampling range available to be displayed on the integrated imaging devices with smaller spatial resolution angle and larger viewing angle.

The EIA2 which matches the parameters of display device can be generated by the proposed EIA resampling method. PA2 is used to capture the reconstructed 3D points, and the parameters of PA2 can be set from that of the display device, and the gap g_2 can be calculated according to the display parameters, as

$$g_2 = \frac{f_2 L_{CDP}}{L_{CDP} - f_2}, \tag{1}$$

where L_{CDP} denotes the gap between PA2 and the central depth plane, f_2 is the focus length of display lens array. The integrated imaging display device works in resolution-priority mode when $g_2 \neq f$, and it works in depth-priority mode when $g_2 = f_2$.

PA2 is used to capture the light rays emitted from the reconstructed object point, and the resampling spacing can be calculated as

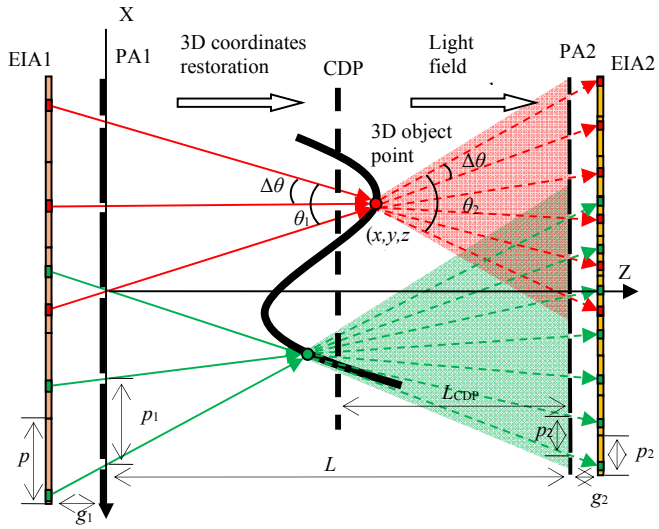

FIGURE I. DIAGRAM OF EIA GENERATION METHOD

$$\Delta\theta_2 = \frac{p_2}{L-z}$$

To avoid the overlap between adjacent elemental images, the light field resampling range must be restricted as

$$\theta_2 \le 2\,\mathrm{atan}\left(\frac{p_2}{2g_2}\right)$$

With the restriction of EIA resampling range θ_2, range of serial numbers of pinhole (m',n') which can capture the light rays of object point can be expressed as

$$\begin{cases} \left|m'p_2 - x\right| \le (L-z)\tan(\theta_2/2) \\ \left|n'p_2 - y\right| \le (L-z)\tan(\theta_2/2) \end{cases}$$

The coordinates $I'(m',n',i',j')$ of the pixel which captures the light rays through pinhole (m', n'), can be written as

$$\begin{cases} i' = [p_2/2 - \dfrac{g_2(m'p_2 - x)}{L-z}]/\Delta p_2 \\ j' = [p_2/2 - \dfrac{g_2(n'p_2 - y)}{L-z}]/\Delta p_2 \end{cases} \quad (5)$$

Equation (5) indicates the pixel in the i'th row of j'th column of the elemental image which locates in the m'th row of n'th column of EIA2 captured the light rays of the object point. Δp_2 is the pixel size of EIA2, m' and n' take the round number in the range restricted by Eq. (4).

Finally the pixel value of EIA2 can be obtained from EIA1 through the pixel mapping algorism,

$$I'(m',n',i',j') = I(m,n,i,j) \quad (6)$$

Fig.2 is the flow diagram of the EIA generation procedure. The adjacent elemental images of EIA1 have many repetitions in pixels when the record lens array has small spacing. To avoid repeat computation, each time before a pixel mapping progress the program that we designed will search for the homologous pixels in the previous elemental images of EIA1. If the homologous pixel is found, it demonstrates this object point has been mapped and we skip to the next pixel. In this way, the executive efficiency of the procedure can be improved significantly.

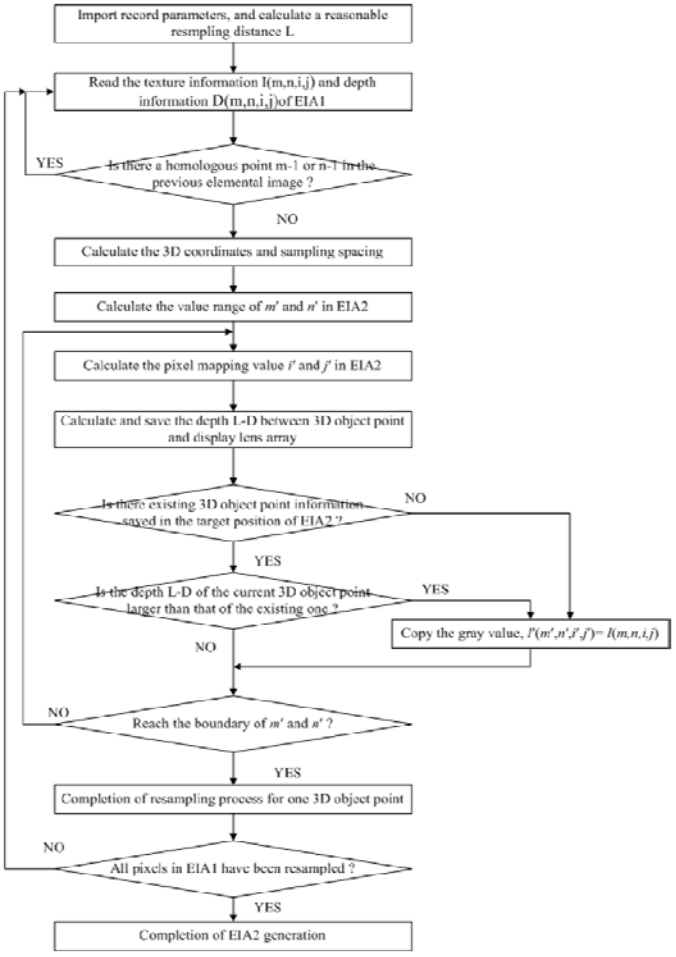

FIGURE II. FLOW DIAGRAM OF THE EIA GENERATION PROCEDURE

III. SIMULATIONS AND RESULTS

We design two integrated imaging display with different parameters, one with macrolens array and the other with microlens array. And then we apply this method to generate the EIA2s which match the two display devices from the EIA1 captured in computer.

A 3D scene we built in software 3DS MAX is shown in Figure 3(a), two characters, '3' and 'D', are set at different depths, a camera array is used to generate the EIA1. The simulation parameters of record device and display device are listed in Table 1.

In the record process, we set up a camera array in 3DS MAX software to record and generate the EIA1 as well as its corresponding depth image, as shown in Figure 3(b) and Figure 3(c). It should be noted that in the recording for a real 3D scene, the texture image and depth image can be recorded by various depth camera (e.g. Kinect) as well.

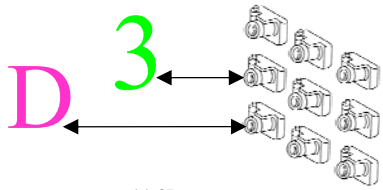

(a) 3D scene

(b) EIA1

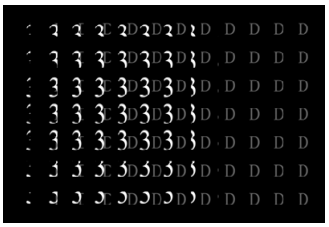

(c) Depth image

FIGURE III. 3D SCENE BUILT IN 3DS MAX SOFTWARE AND PART OF THE EIA1 RECORDED IN COMPUTER.

TABLE I. SIMULATION PARAMETERS OF RECORD DEVICE AND DISPLAY DEVICE

Parameters	**Captured EIA1**	**EIA2 for macrolens array**	**EIA2 for microlens array**
Number of elemental images	$M_1 \times N_1$= 12×7	$M_2 \times N_2$=7×4	$M_2 \times N_2$= 120×67
Pitch of lens array	p_1=10 mm	p_2=14.7mm	p_2=1mm
Focus length of lens array	f_1=15mm	f_2=12.7mm	f_2=3.3mm
Gap between lens array and EIA	g_1=15mm	g_2=14.5mm (resolution-priority mode)	g_2=3.3mm (depth-priority mode)
Resolution of elemental image	r_1=500	r_2=467	r_2=32
Field of view /viewing angle	θ_1=36.87°	θ_2=53.76°	θ_2=17.23°
Gap between record and display lens array	-	L=270mm	L=130mm
Sample spacing of character '3'	$\Delta\theta_1$=5.71°	$\Delta\theta_2$=5.94°	$\Delta\theta_2$=1.91°
Sample spacing of character 'D'	$\Delta\theta_1$=3.37°	$\Delta\theta_2$=8.36°	$\Delta\theta_2$=1.43°

Two sets of EIA2 with different parameters were generated through the proposed EIA generation method, as shown in Figs. 4(a) and 4(b). The generated EIA2s looks very different from the EIA1 shown in Fig. 3(b), and they do not have the problems of pixel mapping errors and homologous pixels missing. According to the computational formula of viewing angle in reference [2], when the EIA2s are displayed on the two integrated imaging system, the viewing angle can be expanded to 53.76° when EIA2 is applied to the display device with macrolens array. The sample spacing of character '3' and 'D' can be decreased to 1.91° and 1.43° respectively when EIA2 is applied to the display device with microlens array, thus a smoother moving parallax can be obtained.

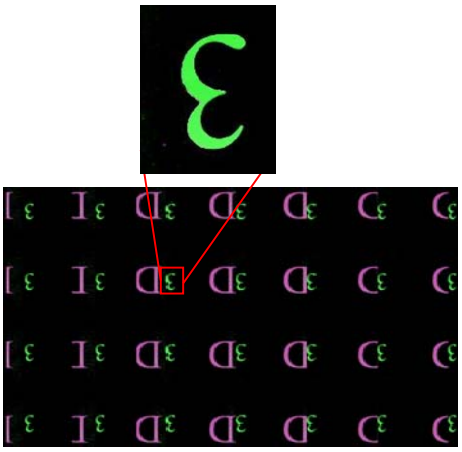

(a) EIA2 ready to be displayed on the integrated imaging system with macrolens array

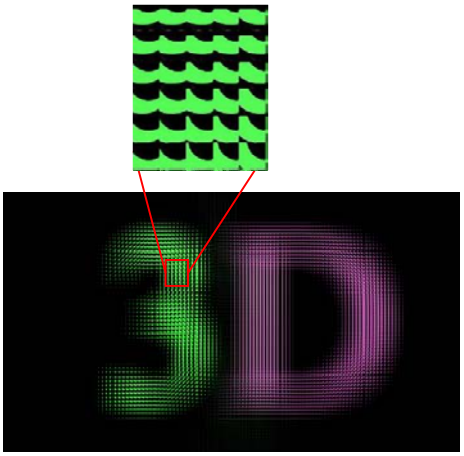

(b) EIA2 ready to be displayed on the integrated imaging system with microlens array

FIGURE IV. TWO EIA2S GENERATED BY OUR PROPOSED METHOD

IV. CONCLUSIONS

We have proposed a 3D source generation method for generating EIA of integrated imaging, by the EIA resampling process. From any given recorded EIA, We can generate a new set of EIA which is suitable to be displayed in an integrated imaging 3D display device. The proposed method can break through the constraints of the field of view and the sampling spacing of record device. We can obtain larger viewing angle or smoother 3D images by generating synthetic EIA with suitable parameters.

ACKNOWLEDGMENT

This work was supported by Innovation project of Chengdu Technological University, No. S201911116059 and Research project of Chengdu Technological University, No. 2019ZR020.

REFERENCES

[1] Y. Piao, M. Zhang, E. S. Kim, S. T. Kim, "Enhanced orthoscopic integral imaging reconstruction using moving pixel mapping," Opt. Laser Eng., vol. 50, pp. 862-868, 2012.

[2] H. Deng, Q. H. Wang, L. Li, D. H. Li. "An integral-imaging three-dimensional display with wide viewing angle," J. Soc. Inf. Display, vol. 19, pp. 679-684, 2011.

[3] Z Wang, A Wang, S Wang, X Ma, H Ming, "Resolution-enhanced integral imaging using two microlens arrays with different focal lengths for capturing and display," Opt. Express, vol. 23, pp. 28970-28977, 2015.

[4] F. Wu, Q. H. Wang, C. G. Luo, D. H. Li, H. Deng, "Dual-view integral imaging 3D display using polarizer parallax barriers," Appl. Opt., vol. 53, pp. 2037-2039, 2014.

[5] G. Lippmann. La photographie integral. "Comptes Rendus de l'Académie des Sciences," vol. 146, pp. 446-451, 1908.

[6] H. E. Ives. "Optical properties of a lippmann lenticulated sheet," J. Opt. Soc. Am. A, vol. 21, pp. 171-176, 1931.

[7] J. Aral, F. Okano, H. Hoshino, I. Yuyama. "Gradient-index lens-array method based on real-time integral photography for three-dimensional images," Appl. Opt., vol. 37, pp. 2034- 2045, 1998.

[8] J. Ser, S. Cha, S. H. Shin, B. Javidi. "Orthoscopic integral imaging 3D display by use of negative lens array," Conference on Lasers and Eletro-Optics, vol. 2, pp. 614, 2003.

[9] J. Wen, X. Yan, X. Jiang, Z. Yan, Y. Wang, J. Wang, "Nonlinear mapping method for the generation of an elemental image array in a photorealistic pseudoscopic free 3D display," Appl. Opt., vol. 57, pp. 6375-6382, 2018.

[10] F. Okano, H. Hoshino, J. Aral, I. Yuyama. "Real-time pickup method for a three-dimensional image based on integral photography," Appl. Opt., vol. 36, pp. 1598-1603, 1997.

[11] J. S. Jang, B. Javidi, "Two-step integral imaging for orthoscopic three-dimensional imaging with improved viewing resolution," Opt. Eng. vol. 41, pp.2568-2571, 2002.

[12] D. H. Shin, B. G. Lee, E. S. Kim , "Modified smart pixel mapping method for displaying orthoscopic 3D images in integral imaging," Opt. Laser Eng., vol. 47, pp. 1189-1194, 2009.

[13] M. Martínez-Corral, A. Dorado, H. Navarro, G. Saavedra, B. Javidi, "Three-dimensional display by smart pseudoscopic-to-orthoscopic conversion with tunable focus," Appl. Opt., vol. 53: E19- E25, 2014.

[14] Z. Yan, X. Jiang, X. Yan, "Performance-improved smart pseudoscopic to orthoscopic conversion for integral imaging by use of lens array shifting technique," Opt. Commun., vol. 420, pp. 157-162, 2018.

[15] H. Navarro, R. Martínez-Cuenca, G. Saavedra, M. Martínez-Corral, and B. Javidi , "3D integral imaging display by smart pseudoscopic-to-orthoscopic conversion (SPOC) ," Opt. Express, vol. 18, pp. 25573-25583, 2010.

[16] H. Deng, Q. H. Wang, D. H. Li, F. N. Wang, "Realization of undistorted and orthoscopic integral imaging without black zone in real and virtual fields," J. Disp. Technol., vol. 7, pp.255-258, 2011.

[17] J. Zhang, Y. Liu, X. Wang, "Method for eliminating the black zone of integral imaging," 10th International Conference on P2P, pp.458-461, 2015.

[18] X. Xiao, X. Shen, M. Martinez-Corral, B. Javidi, "Multiple-planes pseudoscopic-to- orthoscopic conversion for 3D integral imaging display," J. Disp. Technol., vol. 11, pp. 921-926, 2015.